NeuroImage 122 (2015) 440–450

Contents lists available at ScienceDirect

NeuroImage

journal homepage: www.elsevier.com/locate/ynimg

Single-dose serotonergic stimulation shows widespread effects on functional brain connectivity

Bernadet L. Klaassens [a,b,c,d,*], Helene C. van Gorsel [d], Najmeh Khalili-Mahani [e], Jeroen van der Grond [b], Bradley T. Wyman [f], Brandon Whitcher [f], Serge A.R.B. Rombouts [a,b,c], Joop M.A. van Gerven [d]

[a] Leiden University, Institute of Psychology, Leiden, The Netherlands
[b] Leiden University Medical Center, Department of Radiology, Leiden, The Netherlands
[c] Leiden University, Leiden Institute for Brain and Cognition, Leiden, The Netherlands
[d] Centre for Human Drug Research, Leiden, The Netherlands
[e] McGill University, Montreal Neurological Institute, Montreal, QC, Canada
[f] Pfizer Inc., Cambridge, MA, USA

ARTICLE INFO

Article history:
Received 10 April 2015
Accepted 6 August 2015
Available online 12 August 2015

Keywords:
FMRI
Functional connectivity
Neuropharmacology
Resting state networks
SSRI
Serotonin

ABSTRACT

The serotonergic system is widely distributed throughout the central nervous system. It is well known as a mood regulating system, although it also contributes to many other functions. With resting state functional magnetic resonance imaging (RS-fMRI) it is possible to investigate whole brain functional connectivity. We used this non-invasive neuroimaging technique to measure acute pharmacological effects of the selective serotonin reuptake inhibitor sertraline (75 mg) in 12 healthy volunteers. In this randomized, double blind, placebo-controlled, crossover study, RS-fMRI scans were repeatedly acquired during both visits (at baseline and 3, 5, 7 and 9 h after administering sertraline or placebo). Within-group comparisons of voxelwise functional connectivity with ten functional networks were examined ($p < 0.005$, corrected) using a mixed effects model with cerebrospinal fluid, white matter, motion parameters, heart rate and respiration as covariates. Sertraline induced widespread effects on functional connectivity with multiple networks; the default mode network, the executive control network, visual networks, the sensorimotor network and the auditory network. A common factor among these networks was the involvement of the precuneus and posterior cingulate cortex. Cognitive and subjective measures were taken as well, but yielded no significant treatment effects, emphasizing the sensitivity of RS-fMRI to pharmacological challenges. The results are consistent with the existence of an extensive serotonergic system relating to multiple brain functions with a possible key role for the precuneus and cingulate.

Introduction

The central serotonergic system plays an important modulatory role and affects diverse functions like cognition, mood, appetite, sleep and sensorimotor activity. Different classes of serotonin (5-hydroxytryptamine, 5-HT) receptors exist, and they are distributed throughout the whole brain, including the cortex, limbic areas, hypothalamus, basal ganglia, brain stem and cerebellum (Barnes and Sharp, 1999; Carr and Lucki, 2011; Hoyer et al., 2002; Jacobs and Azmitia, 1992; Nichols and Nichols, 2008). The selective serotonin reuptake inhibitor (SSRI) sertraline increases the concentration of synaptic serotonin and is commonly prescribed as a treatment for depression and anxiety disorders (McRae et al., 2001).

Functional brain imaging shows that SSRIs change brain activation and perfusion in limbic and prefrontal regions, which have been identified as important mediators in emotional processing. However, SSRIs also influence many other brain structures, including the precuneus, basal ganglia, brain stem, cerebellum, hypothalamus, temporal, parietal and occipital areas (Anderson et al., 2007; Bruhl et al., 2011; Geday et al., 2005; Klomp et al., 2012; McKie et al., 2005; Smith et al., 2002; Viviani et al., 2012).

Understanding the mechanism of action of the extensive system of serotonergic neurons requires a method for studying large-scale network interactions instead of isolated brain regions (Schaefer et al., 2014). The resting state functional magnetic resonance imaging (RS-fMRI) technique allows an integral non-invasive investigation of these network interactions, taking into account the brain's comprehensive neural circuit (Fox and Raichle, 2007; Lu and Stein, 2014).

The main focus of most RS-fMRI studies on SSRIs has been functional connectivity of the default mode network (DMN), which includes the posterior cingulate, precuneus and medial prefrontal, temporal and parietal regions. The DMN, one of the most consistent networks, is

* Corresponding author at: Leiden University, Institute of Psychology, Unit Methodology and Statistics, PO Box 9555, 2300 RB Leiden, The Netherlands. Fax: +31 71 527 3761.
E-mail address: b.klaassens@lumc.nl (B.L. Klaassens).

http://dx.doi.org/10.1016/j.neuroimage.2015.08.012
1053-8119/

affected in multiple mental disorders, including depression (Sundermann et al., 2014). SSRI administration shows a reduction in functional DMN connectivity, indicating normalization of patterns as seen in depression (Li et al., 2013; McCabe and Mishor, 2011; McCabe et al., 2011; van de Ven et al., 2013; van Wingen et al., 2014). Yet, SSRIs are expected to change functional connections in brain regions beyond the DMN too (Schaefer et al., 2014).

Here, we apply a technique of repeated measures RS-fMRI and an analysis of region-to-network connectivity to study whole brain treatment effects of an SSRI in healthy young volunteers. We have shown the sensitivity of this approach for various other pharmacological challenges (Cole et al., 2013; Khalili-Mahani et al., 2012, 2015; Klumpers et al., 2012; Niesters et al., 2012). Given the widespread distribution of serotonergic receptors in the brain and the involvement of serotonin in many brain functions, we hypothesize that a single-dose of the SSRI sertraline will not only affect the DMN but various resting state brain networks, related to emotional, sensory, motor, cognitive and executive functioning.

Materials and methods

Subjects

Twelve healthy young volunteers (mean age 23.0 ± 2.8, range 19–28; gender ratio 1:1; BMI 19–24 kg/m^2) were recruited to participate in the study. All subjects underwent a thorough medical screening at the Centre for Human Drug Research (CHDR) to investigate whether they met the inclusion and exclusion criteria. They had a normal history of physical and mental health and were able to refrain from using nicotine and caffeine during study days. Other exclusion criteria included positive drug or alcohol screen on study days, regular excessive consumption of alcohol (>4 units/day), caffeine (>6 units/day) or cigarettes (>5 cigarettes/day), use of concomitant medication 2 weeks prior to study participation and involvement in an investigational drug trial 3 months prior to administration. The study was approved by the medical ethics committee of the Leiden University Medical Center (LUMC) and the scientific review board of the CHDR. Written informed consent was obtained from each subject prior to study participation.

Study design

This was a single center, double blind, placebo-controlled, crossover study with sertraline 75 mg. To cover the interval of maximum concentrations of sertraline (T_{max}: 5.5–9.5 h, $T_{1/2}$: 26 h), five RS-fMRI scans were acquired during study days, one at baseline and four after administering sertraline or placebo (at 3, 5, 7 and 9 h post dosing). Each scan was followed by performance of computerized cognitive tasks (taken twice at baseline) on the NeuroCart® test battery, developed by the CHDR for quantifying pharmacological effects on the central nervous system (CNS). By including multiple measurements during the T_{max} interval, this repeated measures profile increases the statistical power of the analysis. Currently, there are no formal power calculation methods that allow estimating the sample size for testing whole brain functional variations. Our sample size was selected based on previous studies (Khalili-Mahani et al., 2012, 2015; Klumpers et al., 2012; Niesters et al., 2012) that demonstrated sufficient power to detect significant effects in repeated measures designs with 12 subjects. Sertraline and placebo were administered orally as capsules, matched for size and weight. To reduce the most common side effect of sertraline (nausea and vomiting), drug treatment was combined with granisetron 2 mg tablets on both study days. Multiple blood samples were taken during the course of the day to define the pharmacokinetic (PK) profile of sertraline in serum, its active metabolite desmethylsertraline and concentrations of cortisol and prolactin. Washout period between the two study days was at least 10 days. An overview of the study design is provided in Fig. 1.

Blood sampling

Pharmacokinetics

Blood samples were collected in 4 mL serum tubes at baseline and 1.5, 3, 5, 6, 7 and 9 h post dosing, centrifuged (2000 *g* for 10 min) and stored at −40 °C until analysis with liquid chromatography–tandem mass spectrometry (LC–MS/MS). PK parameters for sertraline and its active metabolite desmethylsertraline were calculated using a non-compartmental analysis. Maximum serum concentrations (C_{max}) and time of C_{max} (T_{max}) were obtained directly from the serum concentration data. The area under the serum concentration versus time curve was calculated from time zero to the time of the last quantifiable serum measured concentration, which is equal to the last blood sample of the study day (AUC_{0-last}). The calculated PK parameters were not used for further analysis but investigated to validate the choice of time points of measurements.

Neuroendocrine variables

Blood samples were also obtained to determine cortisol and prolactin concentrations. Serum samples were taken in a 3.5 mL gel tube at baseline and 1.5, 3, 5, 6, 7 and 9 h post dosing, centrifuged (2000 *g* for 10 min) and stored at −40 °C until analysis. Serum concentrations were quantitatively determined with electrochemiluminescence immunoassay. Cortisol and prolactin concentrations were subsequently used for statistical analysis using a mixed effects model with treatment, time and treatment by time as fixed effects, subject, subject by treatment and subject by time as random effects and the average of the period baseline (pre-dose) values as covariate (SAS for Windows V9.1.3; SAS Institute, Inc., Cary, NC, USA). In the Results section, significant treatment effects (at $p < 0.05$) will be discussed.

NeuroCart® test battery

Each RS-fMRI scan was followed by functional CNS measures outside the scanner using the computerized NeuroCart® test battery measuring alertness, mood and calmness (Visual Analogue Scales (VAS) Bond & Lader), nausea (VAS Nausea), vigilance and visual motor performance (Adaptive Tracking task), reaction time (Simple Reaction Time task), attention, short-term memory, psychomotor speed, task switching and inhibition (Symbol Digit Substitution Test and Stroop task), working memory (N-back task) and memory imprinting and retrieval plus

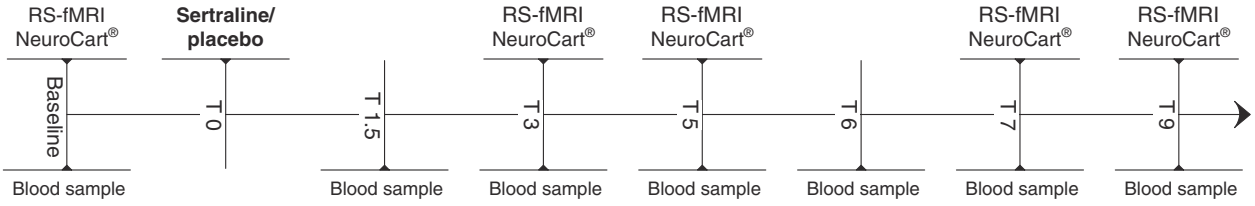

Fig. 1. Schematic presentation of a study day. At baseline, one RS-fMRI scan was acquired, followed by the NeuroCart® CNS test battery (performed twice at baseline). After drug administration, four more RS-fMRI scans were acquired at time points T = 3, 5, 7 and 9 h post dosing, each time followed the NeuroCart® test battery. During the day, seven blood samples were taken to measure the concentrations of (desmethyl)sertraline, cortisol and prolactin.

social processing (Face Encoding and Recognition task) (Bond and Lader, 1974; Borland and Nicholson, 1984; Laeng et al., 2005; Lezak, 2004; Lim et al., 2008; Norris, 1971; Rogers et al., 2004; Stroop, 1935; Wechsler, 1981). The Face Encoding and Recognition task was only performed twice during each day (at baseline and 7 h post dosing) because of limited different test versions. Duration of each series of NeuroCart® brain function tests was approximately 20 min (except for the baseline series when each task was executed twice within approximately 40 min). To minimize learning effects, training for the NeuroCart® tasks occurred during the screening visit within 3 weeks prior to the first study day.

Analysis

All post-dose repeatedly measured CNS endpoints were analyzed using a mixed effects model with treatment, time and treatment by time as fixed effects, subject, subject by treatment and subject by time as random effects and the average of the period baseline (pre-dose) values as covariate (SAS for Windows V9.1.3; SAS Institute, Inc., Cary, NC, USA). As data of the Simple Reaction Time task were not normally distributed, these data were log-transformed before analysis and back transformed after analysis. The data of the Face Encoding and Recognition task were analyzed using a mixed effects model with treatment as fixed effect and subject as random effect and the baseline value as covariate. In the Results section, significant treatment effects (at $p < 0.05$) will be discussed.

Imaging

Scanning was performed at the LUMC on a Philips 3.0 T Achieva MRI scanner (Philips Medical System, Best, The Netherlands) using a 32-channel head coil. During the RS-fMRI scans, all subjects were asked to close their eyes while staying awake. They were also instructed not to move their head during the scan. Instructions were given prior to each scan on both days. T1-weighted anatomical images were acquired once per visit. To facilitate registration to the anatomical image, each RS-fMRI scan was followed by a high-resolution T2*-weighted echo-planar scan. Duration was approximately 8 min for the RS-fMRI scan, 5 min for the anatomical scan and 30 s for the high-resolution scan. Heart rate and respiration signals were recorded during each scan.

RS-fMRI data were obtained with T2*-weighted echo-planar imaging (EPI) with the following scan parameters: 220 whole brain volumes, repetition time (TR) = 2180 ms; echo time (TE) = 30 ms; flip angle = 85°; field-of-view (FOV) = 220 × 220 × 130 mm; in-plane voxel resolution = 3.44 × 3.44 mm, slice thickness = 3.44 mm, including 10% interslice gap. The next parameters were used to collect T1-weighted anatomical images: TR = 9.1 ms; TE = 4.6 ms; flip angle = 8°; FOV = 224 × 117 × 168 mm; in-plane voxel resolution = 1.17 × 1.17 mm; slice thickness = 1.2 mm. Parameters of high-resolution T2*-weighted EPI scans were set to: TR = 2200 ms; TE = 30 ms; flip angle = 80°; FOV = 220 × 220 × 168 mm; in-plane voxel resolution = 1.96 × 1.96 mm; slice thickness = 2.0 mm.

Analysis

All analyses were performed using the Functional Magnetic Resonance Imaging of the Brain (FMRIB) Software Library (FSL, Oxford, United Kingdom) version 5.0.4 (Jenkinson et al., 2012; Smith et al., 2004; Woolrich et al., 2009). Each individual functional EPI image was inspected, brain-extracted and corrected for geometrical displacements due to head movement with linear (affine) image registration. Images were temporally filtered (with a high pass filter of 150 s) and spatially smoothed (with a 6 mm full-width half-maximum Gaussian kernel). Thereafter, scans were co-registered with the brain extracted high resolution T2*-weighted EPI scans (with 6 degrees of freedom) and T1 weighted images (using the Boundary-Based-Registration method) (Greve and Fischl, 2009; Smith, 2002). The T1-weighted scans were non-linearly registered to the MNI 152 standard space (the Montreal Neurological Institute, Montreal, QC, Canada) using FMRIB's Nonlinear Image Registration Tool. Registration parameters were combined to transform fMRI scans into standard space.

After preprocessing, RS-fMRI networks were extracted from each individual RS-fMRI dataset (12 subjects × 2 days × 5 scans = 120 datasets) using a dual regression analysis (Beckmann et al., 2009; Filippini et al., 2009) based on 10 predefined standard network templates. Confound regressors of time series from white matter (measured from the center of the corpus callosum) and cerebrospinal fluid (measured from the center of lateral ventricles) as well as six motion parameters (the estimated translation along and rotation around the x, y and z axes) were included in this analysis to account for non-neuronal signal fluctuations (Birn, 2012). The 10 standard templates (see Fig. 2) have previously been identified using a data-driven approach (Smith et al., 2009) and comprise the following networks: three visual networks (consisting of medial, occipital pole, and lateral visual areas), DMN (medial parietal, bilateral inferior–lateral–parietal and ventromedial frontal cortex), cerebellar network, sensorimotor network (supplementary motor area, sensorimotor cortex, and secondary somatosensory cortex), auditory network (superior temporal gyrus, Heschl's gyrus, and posterior insular), executive control network (medial–frontal areas, including anterior cingulate and paracingulate) and two frontoparietal networks (frontoparietal areas left and right). With the dual regression method, spatial maps representing voxel-to-network connectivity were estimated for each dataset separately in two stages for use in within-group comparisons. First, the weighted network maps were used in a spatial regression into each dataset. This stage generated 12 time series per dataset that describe the average temporal course of signal fluctuations of the 10 networks plus 2 confound regressors (cerebrospinal fluid and white matter). The six motion parameters, as estimated during motion correction, were inserted into the output files of this first stage for further analysis. Next, these time series were entered in a temporal regression into the same dataset. This resulted in a spatial map per network per dataset with regression coefficients referring to the weight of each voxel being associated with the characteristic signal change of a specific network. The higher the value of the coefficient, the stronger the connectivity of this voxel with a given network. These individual statistical maps were subsequently used for higher level analysis.

Within-group comparisons for the contrast sertraline relative to placebo of voxelwise functional connectivity with each of the 10 functional networks were examined with a mixed effects general linear model as used in our previous studies (Khalili-Mahani et al., 2012; Klumpers et al., 2012; Niesters et al., 2012). Average heart rate (beats/m) and respiration frequency (Hz) per RS-fMRI scan were added to the model as confound regressors, indicated as the most robust method to account for physiological variations (Khalili-Mahani et al., 2013). In this model, treatment and time are used as fixed within-subject factors and subject as a random factor. More specifically, the treatment effect of sertraline versus placebo was tested, with the subjects' means, and variance across time (each time point post dosing versus baseline) modeled as covariates of no interest. Nonparametric permutation testing was used to estimate (with 5000 repeated permutations) for each network whether connectivity was significantly different on sertraline relative to placebo days. The resulting voxelwise probability map was corrected for the familywise error using threshold-free cluster enhancement and by Bonferroni correction for the 10 separately investigated networks (by examining the results at $p < 0.005$) (Smith and Nichols, 2009; Winkler et al., 2014).

Results

Pharmacokinetics

The T_{max} of serum sertraline varied between 2.90 and 6.92 h (mean T_{max}: 3.93 ± 1.34) and between 2.90 and 6.92 h (mean T_{max}: 4.01 ± 1.44) for desmethylsertraline. C_{max} for sertraline was between 14.40

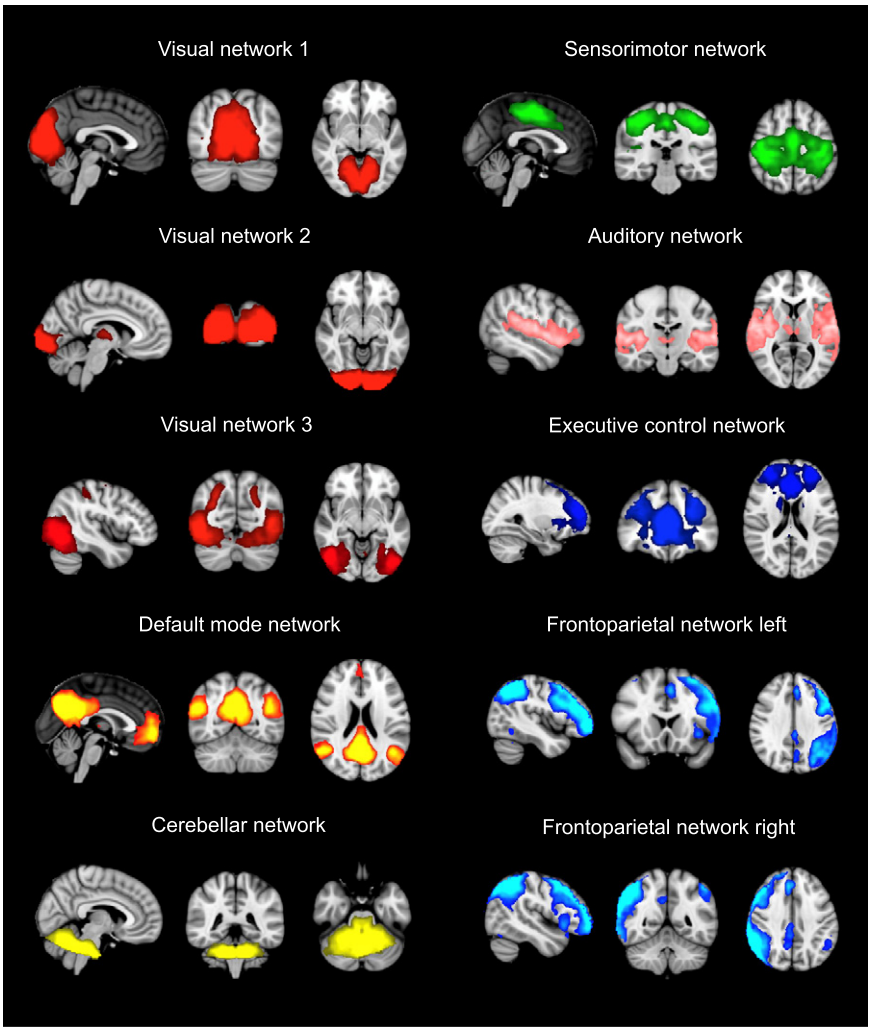

Fig. 2. Ten functional resting state networks as identified by Smith et al. (2009) in 36 healthy adults. To investigate sertraline effects, subject-wise spatial maps of these 10 networks were estimated using dual regression and entered in a mixed effects model for within-group comparisons ($p < 0.005$, corrected).

and 52.80 ng/mL (mean C_{max}: 31.06 ± 11.84) and for desmethylsertraline between 4.50 and 17.10 ng/mL (mean C_{max}: 10.08 ± 3.84). AUC_{0-last} was between 78.17 and 305.60 ng ∗ h/mL (mean AUC_{0-last}: 173.90 ± 69.62) for sertraline and between 5.16 and 98.30 ng ∗ h/mL (mean AUC_{0-last}: 50.75 ± 27.65) for desmethylsertraline (see Fig. 3 for individual and median sertraline PK time profiles).

Cortisol and prolactin

There was a significant treatment effect on concentrations of cortisol (with $F = (1, 10)$ 17.87, $p < 0.01$). As shown in Fig. 4, cortisol concentrations were increased after sertraline, relative to placebo. There was no significant treatment effect for prolactin concentrations.

NeuroCart® test battery

There were no significant treatment effects on measures of cognitive performance. Non-significant trends were found for the VAS Calmness (with $F = (1, 8)$ 5.11, $p = 0.054$: sertraline < placebo), the VAS Mood (with $F = (1, 8)$ 4.12, $p = 0.076$: sertraline < placebo) and the VAS Nausea (with $F = (1, 10)$ 3.84, $p = 0.078$: sertraline > placebo).

Imaging

Functional connectivity changes caused by sertraline were observed in relation to seven functional networks (see Fig. 5 for statistical maps of

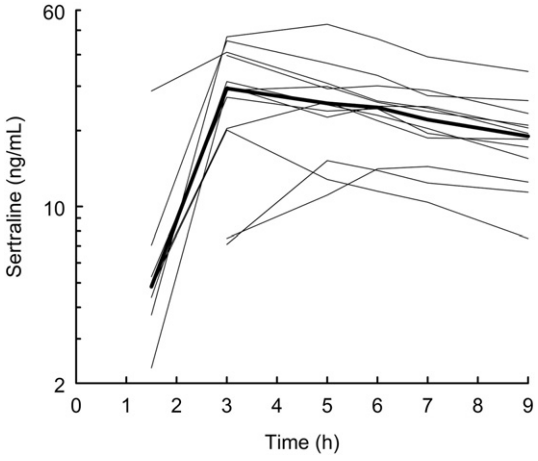

Fig. 3. Median (bold line) and individual (thin lines) pharmacokinetic profiles for sertraline concentrations in nanograms per milliliter on semi-log scale. Observations below limit of quantification were dismissed.

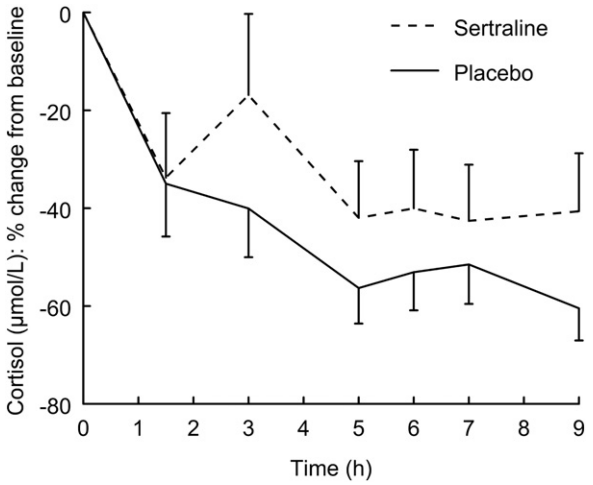

Fig. 4. Least squares means percent change from baseline profiles of cortisol concentrations (with standard errors of the mean as error bars).

the results; $p < 0.005$, corrected). The colors in Fig. 5 match the colors of Fig. 2 with regard to the defined networks. In Fig. 2, the network that was investigated is shown, whereas in Fig. 5, we show the regions in the brain that have altered connectivity with this network. Specifications of effects (cluster size and peak *t*-value of the clusters) are provided in Table 1. Compared to placebo, connections with the following networks were altered after administering sertraline:

Default mode network

Functional connectivity of the anterior cingulate cortex (ACC), posterior cingulate cortex (PCC), medial prefrontal cortex and precuneus (orange in Fig. 5a) with the DMN (orange in Fig. 2) was decreased after sertraline compared to placebo.

Executive control network

Functional connectivity of the limbic system (including the ACC, PCC, thalamus, amygdala and hippocampus), precuneus, midbrain and medial prefrontal cortex (blue in Fig. 5b) with the executive control network (blue in Fig. 2) was decreased after sertraline compared to placebo.

Visual networks

Functional connectivity of the occipital cortex, ACC, PCC, precuneus, medial prefrontal cortex and small parts of the cerebellum (red in Fig. 5c) with the three visual networks (red in Fig. 2) was decreased after sertraline compared to placebo.

Sensorimotor network

Functional connectivity of the ACC, PCC, precuneus, central gyri and supplementary motor cortex (green in Fig. 5d) with the sensorimotor network (green in Fig. 2) was decreased after sertraline compared to placebo.

Auditory network

Functional connectivity was increased between the precuneus and PCC (pink in Fig. 5e) and the auditory network (pink in Fig. 2) after sertraline compared to placebo.

Common regions

For each of these networks, treatment effects were found in two common areas: the precuneus and PCC. In Fig. 6 these effects are shown for each network in their corresponding color with the precuneus and PCC depicted in pale brown. Regions of effect within the precuneus and PCC were chosen to visualize the time profiles of changes in connectivity in relation to the networks (Fig. 6a–e).

Discussion

Sertraline induced widespread alterations in functional connectivity with multiple resting state networks in the brain. In line with Schaefer et al. (2014) these alterations were primarily decreases in connectivity. Effects in the DMN, executive control network and limbic-frontal circuitry are mostly in agreement with earlier RS-fMRI studies on SSRI effects (Li et al., 2013; McCabe and Mishor, 2011; McCabe et al., 2011; van de Ven et al., 2013; van Wingen et al., 2014). New findings were a lowering of connectivity within visual networks and alterations in functional connectivity of the sensorimotor and auditory network with the cingulate cortex and precuneus. The PK time profile was consistent with our repeated measures, taken at appropriate time points when the largest effects could be expected. Post hoc investigation of connectivity changes over time suggests that sertraline might sometimes suppress regular diurnal fluctuations, similar to the effect we found on cortisol. Consistent with other literature, cortisol concentrations were slightly higher after SSRI administration (Sagud et al., 2002; von Bardeleben et al., 1989), as opposed to a gradual decrease during placebo days. The paucity of effects on cognitive performance implies that RS-fMRI is highly sensitive and appropriate as a measure of a serotonergic challenge when compared to neuropsychological testing.

Default mode and executive control network

Connectivity within the DMN (precuneus, ACC, PCC and medial prefrontal cortex) was decreased after exposure to sertraline. Furthermore, administration of sertraline led to decreased connectivity between the executive control network and the limbic system (including cingulate cortex, amygdala, hippocampus and thalamus), medial prefrontal cortex and the midbrain. The midbrain's median and dorsal raphe nuclei are the major source of serotonin release to the cerebral cortex, especially to the forebrain (Daubert and Condron, 2010; Jacobs and Azmitia, 1992) and are therefore considered to play an important role in SSRI enhancement (Adell et al., 2002; Morgane et al., 2005). The desirable effects of SSRIs on mood are hypothesized to be mainly due to improved functionality and regulation of 5-HT_{1A} (concentrated in the limbic system, especially the hippocampus, cortical areas as the cingulate and raphe nuclei) and 5-$HT_{2A/C}$ (represented in the limbic system, cortex, basal ganglia and choroid plexus) receptors (Barnes and Sharp, 1999; Celada et al., 2013; Daubert and Condron, 2010; Hoyer et al., 2002; McRae et al., 2001). Inhibitory 5-HT_{1A} receptors have a higher affinity for 5-HT than excitatory 5-HT_2 receptors (Peroutka and Snyder, 1979). Consequently, the net result of elevation of serotonin is a reduction of serotonergic activity at low concentrations, followed by stimulation at higher levels. Furthermore, after acute SSRI administration, serotonin reuptake inhibition is attenuated by activation of 5-HT_{1A} autoreceptors in the raphe nuclei, causing inhibition of cell firing (Briley and Moret, 1993). The relatively limited pharmacological effect of a single 75 mg dose of sertraline could explain the decrease in functional connectivity that we found in many parts of the brain. However, compared to our healthy subjects, it is likely that the sensitivity of 5-HT receptors differs in depressed patients and changes with prolonged antidepressant treatment (Whale et al., 2001). The effects on both networks point to alterations in limbic and frontal brain areas. Together, these regions have been regarded as related to emotional functioning and processing (Joseph, 1992), with deficits in the fronto-limbic circuitry shown in depressed patients (Anand et al., 2005; Mayberg, 1997; Seminowicz et al., 2004). Administering SSRIs might correct dysfunction of the fronto-limbic pathways as seen in depression (Hensler, 2006), thereby influencing emotional and motivational information processing and integration. Interestingly, we found changes in connectivity with the precuneus and PCC for all five networks, both part of the DMN and mentioned as playing a central role in self-consciousness and self-reference (Fransson and Marrelec, 2008). The majority of previous RS-fMRI studies point to increased

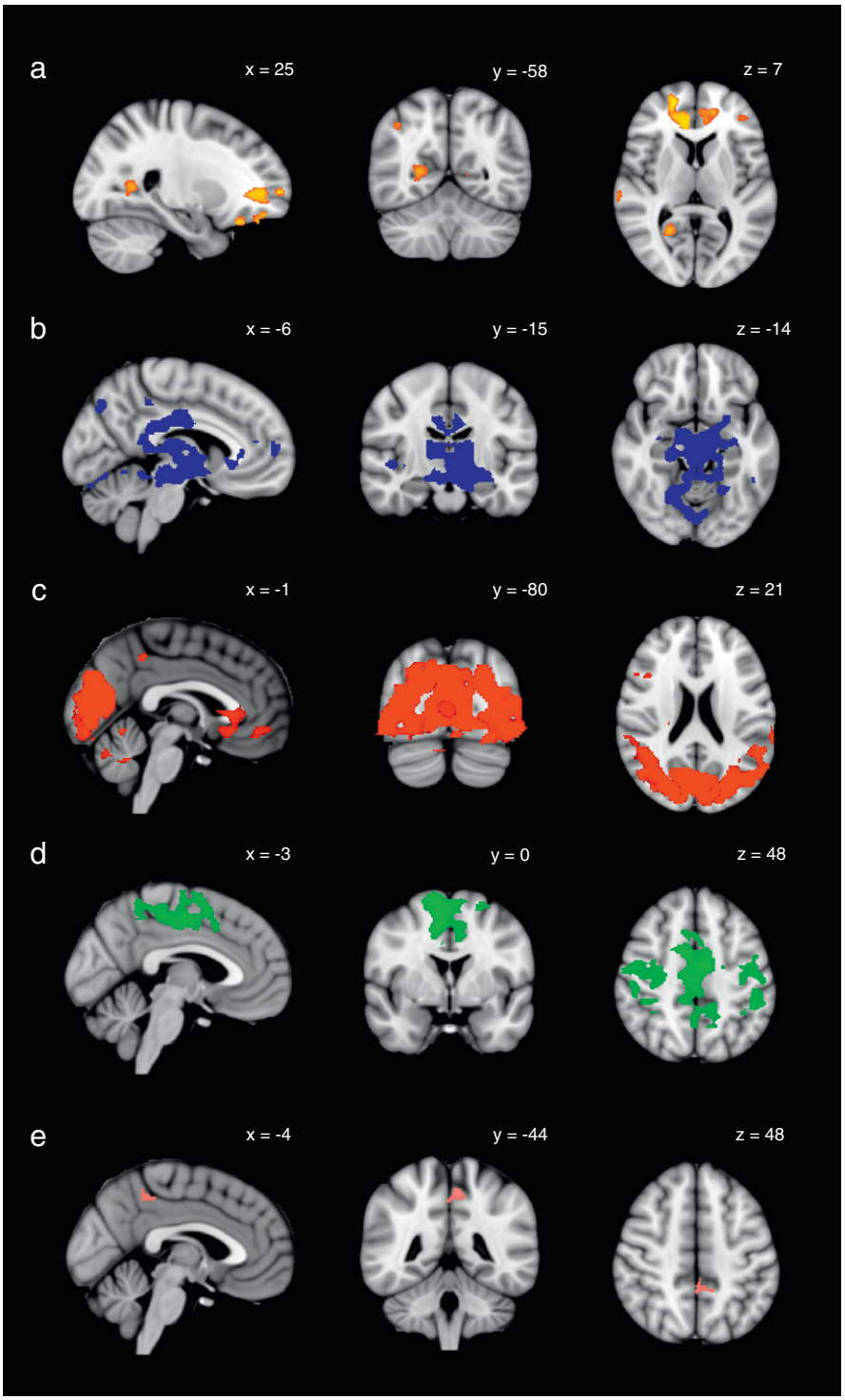

Fig. 5. Spatial maps (with coordinates in mm) of sertraline-induced (a) decreases in functional connectivity between the ACC, PCC, precuneus and medial prefrontal cortex (orange) and the default mode network; (b) decreases in functional connectivity between the limbic system, precuneus, medial prefrontal cortex and midbrain (blue) and the executive control network; (c) decreases in functional connectivity between the occipital cortex, PCC, ACC, precuneus, medial prefrontal cortex and cerebellum (red) and the visual networks; (d) decreases in functional connectivity between the ACC, PCC, precuneus, central gyri and supplementary motor cortex (green) and the sensorimotor network; (e) increases in functional connectivity between the PCC and precuneus (pink) and the auditory network ($p < 0.005$, corrected). Coronal and axial slices are displayed in radiological convention (left = right).

connectivity in depression, particularly of cortical midline structures as the precuneus, ACC and PCC with prefrontal areas (Sundermann et al., 2014). The deviant pattern of the overactivated DMN, supporting internal mentation and integration of experiences, might refer to rumination; heightened self-awareness and -preoccupation during rest (Hamilton et al., 2011; Sheline et al., 2010; Zhu et al., 2012). The effects that we observed include the sub- and perigenual ACC which are particularly associated with rumination (Zhu et al., 2012). The posterior parts of the DMN have been proposed as specific regions where normalization of abnormal activity and functional connectivity takes place after SSRI treatment (Greicius et al., 2007; Kraus et al., 2014; Li et al., 2013).

Table 1
Overview of significant decreases and increases in functional connectivity as estimated with threshold-free cluster enhancement ($p < 0.005$, corrected).

Network	Region (Harvard–Oxford)	t^*	x	y	z	Cluster size
Default mode network	B/M ACC, frontal pole (including frontal medial cortex, paracingulate gyrus)	5.28	16	42	−18	2703
	R inferior and middle frontal gyrus	5.33	46	26	32	1060
	R parahippocampal gyrus	4.74	−14	−10	−30	273
	L ACC, paracingulate gyrus	4.56	−12	46	4	193
	R PCC, precuneus cortex	5.31	24	−56	6	100
	R posterior superior temporal gyrus	4.89	66	−26	6	96
	R pre- and postcentral gyrus	3.96	36	−20	40	90
	R angular gyrus, posterior supramarginal gyrus	4.57	38	−50	34	83
	L frontal pole	4.86	−44	40	2	82
Executive control network	B/M limbic system (including amygdala, hippocampus, thalamus), temporal pole, PCC, midbrain	6.24	52	12	−4	11,381
	L/M superior lateral occipital cortex, cuneal cortex, precuneus cortex	4.13	−18	−62	42	432
	M ACC, frontal medial cortex	4.4	−2	24	−2	295
	R PCC, precuneus cortex	4.77	16	−56	32	243
	L frontal pole (including frontal medial cortex, paracingulate gyrus)	4.65	−8	56	6	140
Visual network 1	B/M occipital cortex (including fusiform gyrus, lingual gyrus, intra- and supracalcarine cortex, cuneal cortex extending into precuneus cortex)	5.55	−18	−68	−4	6592
Visual network 2	B/M occipital cortex (including fusiform gyrus, lingual gyrus, calcarine cortex, cuneal cortex)	5.46	−2	−86	−12	1463
Visual network 3	B lateral occipital, frontal, temporal and parietal cortex, cerebellum, PCC, precuneus cortex, pre- and postcentral gyrus	5.78	20	−80	26	28,546
	B ACC, paracingulate gyrus, subcallosal cortex, frontal medial cortex	5.05	34	42	−2	3757
	R ACC, PCC, precentral gyrus, (middle and superior) frontal gyrus	4.59	12	−10	38	331
	L precentral gyrus, (middle and superior) frontal gyrus	4.96	−30	2	46	111
Sensorimotor network	B/M ACC, PCC, precuneus cortex, supplementary motor area, pre- and postcentral gyrus	7.26	8	2	60	9262
	L ACC, paracingulate gyrus	4.2	−8	26	26	112
Auditory network	B PCC, precuneus cortex, pre- and postcentral gyrus	4.48	−6	−44	52	125

Abbreviations: L = left, R = right, B = bilateral, M = midline, ACC = anterior cingulate cortex, PCC = posterior cingulate cortex. Voxel dimension = 2 mm × 2 mm × 2 mm (voxel volume 0.008 mL). * = uncorrected peak *t*-value within cluster.

Visual, auditory and sensorimotor networks

In the cortex, the frontal lobe contains the highest density of 5-HT terminals, but the midbrain's raphe nuclei project to all other cortical areas as well. High cortical concentrations of serotonin have been found in the primary visual, auditory and somatosensory cortices of primates (Kahkonen et al., 2002; Lidow et al., 1989a; Morrison et al., 1982; Thompson et al., 1994). The relative predominance of high affinity 5-HT_{1A} versus low affinity 5-HT_2 receptors has been demonstrated in the prefrontal cortex (Amargos-Bosch et al., 2004; Celada et al., 2013) but also in the visual and motor cortex of rhesus monkeys (Lidow et al., 1989b). Again, this might explain the observed decrease in functional connectivity of the visual and sensorimotor networks after administering sertraline. Evidence for functional involvement of serotonin in the human visual system comes from observations in users of ecstasy (or 3,4-methylenedioxy-N-methylamphetamine; MDMA). MDMA induces an acute release and reuptake inhibition of serotonin, followed by serotonin depletion in the visual cortex, which is associated with changes in visual orientation processing (Oliveri and Calvo, 2003). Moreover, the 5-HT neuronal activity pattern seems to correspond to and facilitate tonic motor output in animals (Jacobs and Fornal, 1999). We found decreased connectivity of the sensorimotor network with the central gyri (the sensorimotor region) and the supplementary motor area. Improvement of motor behavior after giving SSRIs has been shown with task-related fMRI studies, accompanied by enhancement of brain motor activity in the sensorimotor cortex and supplementary motor area (Loubinoux et al., 2002a, b). Connectivity of the sensorimotor network and visual networks with the precuneus and (para)cingulate cortex was decreased in our study. The cingulate motor areas operate in concert with the limbic system for spatial orientation and executing voluntary movement (Shima and Tanji, 1998; Vogt et al., 1992). The precuneus has been identified as a major association area guiding visuo-spatial imagery, execution and preparation of complex motor behavior and attentive tracking (Cavanna and Trimble, 2006; Zhang and Li, 2012). Connectivity of the precuneus and cingulate cortex with the auditory network was altered as well, although this time it concerned an increase instead of a decrease in connectivity. This corresponds to reverse findings in depression of Sundermann et al. (2014), who observed hypoconnectivity in areas that belong to the auditory network (left temporal cortex, insula). SSRIs have been used for treatment of tinnitus, the perception of a phantom sound (Robinson, 2007). FMRI studies on resting state connectivity in tinnitus patients illustrate the interplay between tinnitus and the auditory network, the DMN and limbic areas (Burton et al., 2012; Kim et al., 2012; Maudoux et al., 2012a, b; Ueyama et al., 2013). For example, the connectivity pattern of the precuneus/PCC region was discovered as positively correlating with emotional distress as measured with the tinnitus handicap inventory (Maudoux et al., 2012b).

NeuroCart® test battery

Compared to placebo, sertraline did not result in any significant treatment effects on neurocognitive tasks of the NeuroCart® battery. There was a trend towards increasing nausea, decreasing calmness and decreasing mood on the VAS. The small size of our sample might be an explanation for the absence of behavioral effects. However, we did detect significant and large-scale effects on resting state connectivity, indicating the suitability of this method as a marker of efficacy compared to cognitive measures. These results suggest that RS-fMRI could be a useful technique in early CNS drug development, which generally requires the use of sensitive methods in relatively small study groups. Performance tasks are known to show limited and inconsistent effects after single acute dosing of an SSRI in healthy subjects (Dumont et al., 2005), although we did not include tests that are potentially more sensitive to SSRIs as EEG recordings, REM-sleep and flicker discrimination tests (Dumont et al., 2005; Rijnbeek et al., 2002). In task-related fMRI paradigms it was shown that acute neural changes take place in the limbic system and prefrontal circuitry (Bruhl et al., 2010; Del-Ben et al., 2005; Murphy et al., 2009; Outhred et al., 2013). Despite the instant neural changes after administration of an SSRI, improvements in mood and cognition usually begin only after a few weeks (Frazer and Benmansour, 2002; Harmer et al., 2009). One explanation for this apparent discrepancy is the acute effect of SSRIs on emotional bias (Bhagwagar et al., 2004; Browning et al., 2007; Harmer et al., 2003a, b), which could increase positive information processing, thereby slowly contributing to resolution of the depression (Harmer, 2008). Since the

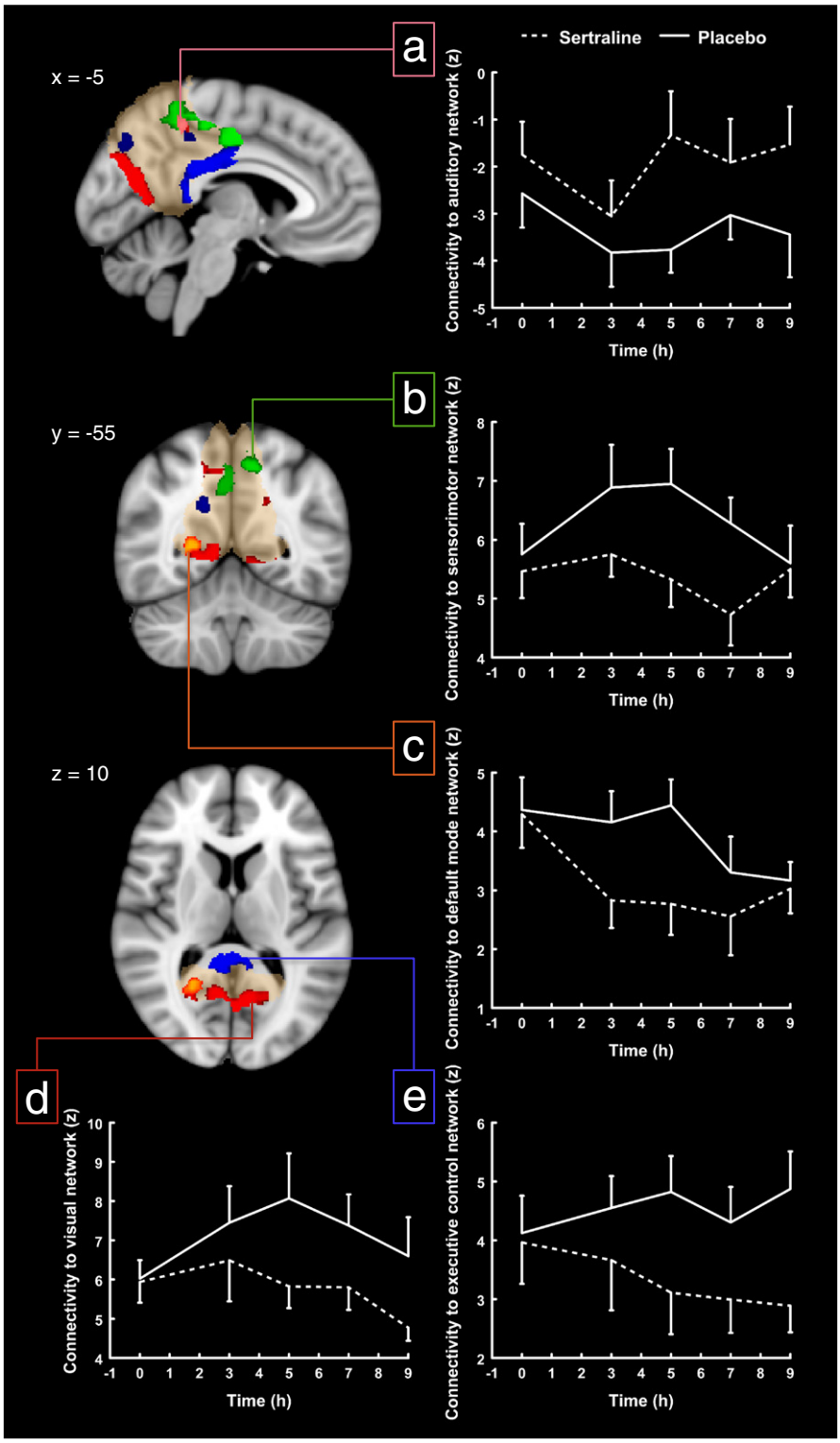

Fig. 6. Alterations in functional connectivity after sertraline administration within the precuneus and PCC (shown in pale brown) for the different networks. Plots visualize the corresponding average time profiles of changes in functional connectivity for sertraline (dotted line) and placebo (continuous line) conditions for (a) the auditory network; (b) the sensorimotor network; (c) the default mode network; (d) the medial visual network; (e) the executive control network (*z*-values with standard errors of the mean as error bars). Coronal and axial slices are displayed in radiological convention (left = right).

Face Encoding and Recognition task involves eliciting emotions, it was expected that an SSRI would exert the strongest acute effect on this task. Contrary to previous literature, we did not find such an effect in this study.

Limitations

Sertraline can be considered as one of the most selective SSRIs. Nevertheless, it still modulates catecholaminergic neurotransmission to

some extent and noradrenergic and dopaminergic influences on functional connectivity cannot be ruled out. Sertraline is especially known for a low relative selectivity for 5-HT over dopamine (Carrasco and Sandner, 2005). The most common side effect during sertraline study days was nausea, which was reported by 50% of the subjects and lasted between 1.5 and 5 h, although this was never severe enough to lead to vomiting. This coincides with a non-significant trend towards experienced nausea on the VAS. Granisetron was added to prevent nausea and vomiting (Jacobs et al., 2010a), which as a side effect of sertraline could have altered the network responses or reduced the tolerability of the procedures (Jacobs et al., 2010b). To balance the study, granisetron was also administrated on placebo days. However, granisetron, being a very selective 5-HT_3 receptor antagonist, might have affected some central serotonergic effects of sertraline that are specifically related to 5-HT_3 functions (Jacobs and Azmitia, 1992). Cortisol influences functional connectivity between the amygdala and medial prefrontal cortex, which might have confounded the results as well (Veer et al., 2012). It is possible that the effects that were found in these areas are partially secondary to the small but significant increase in cortisol concentrations. Moreover, SSRIs potentially affect constriction of blood vessels (Reynell and Harris, 2013) and as a consequence induce blood oxygen level dependent signal changes. This study cannot resolve the question whether observed fMRI effects reflect true neural changes or altered neurovascular coupling (Rack-Gomer et al., 2009; Rack-Gomer and Liu, 2012; Wong et al., 2012). Yet, SSRIs do not typically influence the hemodynamic response (Feczko et al., 2012) and in our study we did not find significant effects of sertraline on heart rate and respiration frequency, which would be considered the main source of causing vascular artifacts.

Conclusions and future perspectives

Using 10 different networks in a well-powered repeated measures design allowed us to confirm both earlier established hypotheses and to discover new, uninvestigated effects of SSRIs on resting state connectivity. The results verify that serotonergic tracts cover a substantial part of the brain and suggest that serotonin is implicated in processing emotional information, conscious coordination of motor behavior and higher-level perception of the environment, possibly with a central role for the precuneus and cingulate. Many network effects of sertraline showed a striking overlap with opposing connectivity changes that are reported in depression (Sundermann et al., 2014). Confirmation of these outcomes will strengthen the confidence in this technique as a highly sensitive and specific method of drug investigation, which in the future may also be used to characterize new drugs under development.

Acknowledgments

This project was funded by the Netherlands Initiative Brain and Cognition (NIHC), a part of the Netherlands Organization for Scientific Research (NWO) (grant number 056-13-016), and Pfizer Inc. Erica Klaassen (CHDR), Jules Heuberger (CHDR) and Pieter Buur (LUMC) are acknowledged for their contribution to statistical analyses.

References

Adell, A., Celada, P., Abellan, M.T., Artigas, F., 2002. Origin and functional role of the extracellular serotonin in the midbrain raphe nuclei. Brain Res. Rev. 39 (2–3), 154–180.
Amargos-Bosch, M., Bortolozzi, A., Puig, M.V., Serrats, J., Adell, A., Celada, P., Toth, M., Mengod, G., Artigas, F., 2004. Co-expression and in vivo interaction of serotonin1A and serotonin2A receptors in pyramidal neurons of prefrontal cortex. Cereb. Cortex 14 (3), 281–299.
Anand, A., Li, Y., Wang, Y., Wu, J.W., Gao, S.J., Bukhari, L., Mathews, V.P., Kalnin, A., Lowe, M.J., 2005. Activity and connectivity of brain mood regulating circuit in depression: a functional magnetic resonance study. Biol. Psychiatry 57 (10), 1079–1088.
Anderson, I.M., Del-Ben, C.M., Mckie, S., Richardson, P., Williams, S.R., Elliott, R., Deakin, J.F.W., 2007. Citalopram modulation of neuronal responses to aversive face emotions: a functional MRI study. Neuroreport 18 (13), 1351–1355.
Barnes, N.M., Sharp, T., 1999. A review of central 5-HT receptors and their function. Neuropharmacology 38 (8), 1083–1152.
Beckmann, C.F., Mackay, C.E., Filippini, N., Smith, S.M., 2009. Group Comparison of Resting-state FMRI Data Using Multi-subject ICA and Dual Regression. OHBM.
Bhagwagar, Z., Cowen, P.J., Goodwin, G.M., Harmer, C.J., 2004. Normalization of enhanced fear recognition by acute SSRI treatment in subjects with a previous history of depression. Am. J. Psychiatry 161 (1), 166–168.
Birn, R.M., 2012. The role of physiological noise in resting-state functional connectivity. NeuroImage 62 (2), 864–870.
Bond, A., Lader, M., 1974. Use of analog scales in rating subjective feelings. Br. J. Med. Psychol. 47 (3), 211–218.
Borland, R.G., Nicholson, A.N., 1984. Visual motor coordination and dynamic visual-acuity. Br. J. Clin. Pharmacol. 18 (Suppl. 1), S69–S72.
Briley, M., Moret, C., 1993. Neurobiological mechanisms involved in antidepressant therapies. Clin. Neuropharmacol. 16 (5), 387–400.
Browning, M., Reid, C., Cowen, P.J., Goodwin, G.M., Harmer, C.J., 2007. A single dose of citalopram increases fear recognition in healthy subjects. J. Psychopharmacol. 21 (7), 684–690.
Bruhl, A.B., Kaffenberger, T., Herwig, U., 2010. Serotonergic and noradrenergic modulation of emotion processing by single dose antidepressants. Neuropsychopharmacology 35 (2), 521–533.
Bruhl, A.B., Jancke, L., Herwig, U., 2011. Differential modulation of emotion processing brain regions by noradrenergic and serotonergic antidepressants. Psychopharmacology 216 (3), 389–399.
Burton, H., Wineland, A., Bhattacharya, M., Nicklaus, J., Garcia, K.S., Piccirillo, J.F., 2012. Altered networks in bothersome tinnitus: a functional connectivity study. BMC Neurosci. 13 (3).
Carr, G.V., Lucki, I., 2011. The role of serotonin receptor subtypes in treating depression: a review of animal studies. Psychopharmacology 213 (2–3), 265–287.
Carrasco, J.L., Sandner, C., 2005. Clinical effects of pharmacological variations in selective serotonin reuptake inhibitors: an overview. Int. J. Clin. Pract. 59 (12), 1428–1434.
Cavanna, A.E., Trimble, M.R., 2006. The precuneus: a review of its functional anatomy and behavioural correlates. Brain 129, 564–583.
Celada, P., Puig, M.V., Artigas, F., 2013. Serotonin modulation of cortical neurons and networks. Front. Integr. Neurosci. 7 (25).
Cole, D.M., Beckmann, C.F., Oei, N.Y.L., Both, S., van Gerven, J.M.A., Rombouts, S.A.R.B., 2013. Differential and distributed effects of dopamine neuromodulations on resting-state network connectivity. NeuroImage 78, 59–67.
Daubert, E.A., Condron, B.G., 2010. Serotonin: a regulator of neuronal morphology and circuitry. Trends Neurosci. 33 (9), 424–434.
Del-Ben, C.M., Deakin, J.F.W., Mckie, S., Delvai, N.A., Williams, S.R., Elliott, R., Dolan, M., Anderson, I.M., 2005. The effect of citalopram pretreatment on neuronal responses to neuropsychological tasks in normal volunteers: an fMRI study. Neuropsychopharmacology 30 (9), 1724–1734.
Dumont, G.J.H., de Visser, S.J., Cohen, A.F., van Gerven, J.M.A., 2005. Biomarkers for the effects of selective serotonin reuptake inhibitors (SSRIs) in healthy subjects. Br. J. Clin. Pharmacol. 59 (5), 495–510.
Feczko, E., Miezin, F.M., Constantino, J.N., Schlaggar, B.L., Petersen, S.E., Pruett, J.R., 2012. The hemodynamic response in children with simplex autism. Dev. Cogn. Neurosci. 2 (4), 396–408.
Filippini, N., MacIntosh, B.J., Hough, M.G., Goodwin, G.M., Frisoni, G.B., Smith, S.M., Matthews, P.M., Beckmann, C.F., Mackay, C.E., 2009. Distinct patterns of brain activity in young carriers of the APOE-epsilon 4 allele. Proc. Natl. Acad. Sci. U.S.A. 106 (17), 7209–7214.
Fox, M.D., Raichle, M.E., 2007. Spontaneous fluctuations in brain activity observed with functional magnetic resonance imaging. Nat. Rev. Neurosci. 8 (9), 700–711.
Fransson, P., Marrelec, G., 2008. The precuneus/posterior cingulate cortex plays a pivotal role in the default mode network: evidence from a partial correlation network analysis. NeuroImage 42 (3), 1178–1184.
Frazer, A., Benmansour, S., 2002. Delayed pharmacological effects of antidepressants. Mol. Psychiatry 7 (Suppl. 1), S23–S28.
Geday, J., Hermansen, F., Rosenberg, R., Smith, D.F., 2005. Serotonin modulation of cerebral blood flow measured with positron emission tomography (PET) in humans. Synapse 55 (4), 224–229.
Greicius, M.D., Flores, B.H., Menon, V., Glover, G.H., Solvason, H.B., Kenna, H., Reiss, A.L., Schatzberg, A.F., 2007. Resting-state functional connectivity in major depression: abnormally increased contributions from subgenual cingulate cortex and thalamus. Biol. Psychiatry 62 (5), 429–437.
Greve, D.N., Fischl, B., 2009. Accurate and robust brain image alignment using boundary-based registration. NeuroImage 48 (1), 63–72.
Hamilton, J.P., Furman, D.J., Chang, C., Thomason, M.E., Dennis, E., Gotlib, I.H., 2011. Default-mode and task-positive network activity in major depressive disorder: implications for adaptive and maladaptive rumination. Biol. Psychiatry 70 (4), 327–333.
Harmer, C.J., 2008. Serotonin and emotional processing: does it help explain antidepressant drug action? Neuropharmacology 55 (6), 1023–1028.
Harmer, C.J., Bhagwagar, Z., Perrett, D.I., Vollm, B.A., Cowen, P.J., Goodwin, G.M., 2003a. Acute SSRI administration affects the processing of social cues in healthy volunteers. Neuropsychopharmacology 28 (1), 148–152.
Harmer, C.J., Hill, S.A., Taylor, M.J., Cowen, P.J., Goodwin, G.M., 2003b. Toward a neuropsychological theory of antidepressant drug action: increase in positive emotional bias after potentiation of norepinephrine activity. Am. J. Psychiatry 160 (5), 990–992.
Harmer, C.J., Goodwin, G.M., Cowen, P.J., 2009. Why do antidepressants take so long to work? A cognitive neuropsychological model of antidepressant drug action. Br. J. Psychiatry 195 (2), 102–108.
Hensler, J.G., 2006. Serotonergic modulation of the limbic system. Neurosci. Biobehav. Rev. 30 (2), 203–214.

Hoyer, D., Hannon, J.P., Martin, G.R., 2002. Molecular, pharmacological and functional diversity of 5-HT receptors. Pharmacol. Biochem. Behav. 71 (4), 533–554.
Jacobs, B.L., Azmitia, E.C., 1992. Structure and function of the brain–serotonin system. Physiol. Rev. 72 (1), 165–229.
Jacobs, B.L., Fornal, C.A., 1999. Activity of serotonergic neurons in behaving animals. Neuropsychopharmacology 21 (Suppl. 2), S9–S15.
Jacobs, G.E., Kamerling, I.M.C., de Kam, M.L., DeRijk, R.H., van Pelt, J., Zitman, F.G., van Gerven, J.M.A., 2010a. Enhanced tolerability of the 5-hydroxytryptophane challenge test combined with granisetron. J. Psychopharmacol. 24 (1), 65–72.
Jacobs, G.E., van der Grond, J., Teeuwisse, W.M., Langeveld, T.J.C., van Pelt, J., Verhagen, J.C.M., de Kam, M.L., Cohen, A.F., Zitman, F.G., van Gerven, J.M.A., 2010b. Hypothalamic glutamate levels following serotonergic stimulation: a pilot study using 7-Tesla magnetic resonance spectroscopy in healthy volunteers. Prog. Neuro-Psychopharmacol. Biol. Psychiatry 34 (3), 486–491.
Jenkinson, M., Beckmann, C.F., Behrens, T.E., Woolrich, M.W., Smith, S.M., 2012. FSL. NeuroImage 62, 782–790.
Joseph, R., 1992. The limbic system — emotion, laterality, and unconscious mind. Psychoanal. Rev. 79 (3), 405–456.
Kahkonen, S., Ahveninen, J., Pennanen, S., Liesivuori, J., Ilmoniemi, R.J., Jaaskelainen, I.P., 2002. Serotonin modulates early cortical auditory processing in healthy subjects. Evidence from MEG with acute tryptophan depletion. Neuropsychopharmacology 27 (5), 862–868.
Khalili-Mahani, N., Zoethout, R.M.W., Beckmann, C.F., Baerends, E., de Kam, M.L., Soeter, R.P., Dahan, A., van Buchem, M.A., van Gerven, J.M.A., Rombouts, S.A.R.B., 2012. Effects of morphine and alcohol on functional brain connectivity during "resting state": a placebo-controlled crossover study in healthy young men. Hum. Brain Mapp. 33 (5), 1003–1018.
Khalili-Mahani, N., Chang, C., van Osch, M.J., Veer, I.M., van Buchem, M.A., Dahan, A., Beckmann, C.F., van Gerven, J.M.A., Rombouts, S.A.R.B., 2013. The impact of "physiological correction" on functional connectivity analysis of pharmacological resting state fMRI. NeuroImage 65, 499–510.
Khalili-Mahani, N., Niesters, M., van Osch, M.J., Oitzl, M., Veer, I., de Rooij, M., van Gerveng, J., van Buchem, M.A., Beckmann, C.F., Rombouts, S.A.R.B., Dahan, A., 2015. Ketamine interactions with biomarkers of stress: a randomized placebo-controlled repeated measures resting-state fMRI and PCASL pilot study in healthy men. NeuroImage 108, 396–409.
Kim, J.Y., Kim, Y.H., Lee, S., Seo, J.H., Song, H.J., Cho, J.H., Chang, Y., 2012. Alteration of functional connectivity in tinnitus brain revealed by resting-state fMRI?: a pilot study. Int. J. Audiol. 51 (5), 413–417.
Klomp, A., Caan, M.W.A., Denys, D., Nederveen, A.J., Reneman, L., 2012. Feasibility of ASL-based phMRI with a single dose of oral citalopram for repeated assessment of serotonin function. NeuroImage 63 (3), 1695–1700.
Klumpers, L.E., Cole, D.M., Khalili-Mahani, N., Soeter, R.P., te Beek, E.T., Rombouts, S.A.R.B., van Gerven, J.M.A., 2012. Manipulating brain connectivity with delta(9)-tetrahydrocannabinol: a pharmacological resting state FMRI study. NeuroImage 63 (3), 1701–1711.
Kraus, C., Ganger, S., Losak, J., Hahn, A., Savli, M., Kranz, G.S., Baldinger, P., Windischberger, C., Kasper, S., Lanzenberger, R., 2014. Gray matter and intrinsic network changes in the posterior cingulate cortex after selective serotonin reuptake inhibitor intake. NeuroImage 84, 236–244.
Laeng, B., Lag, T., Brennen, T., 2005. Reduced stroop interference for opponent colors may be due to input factors: evidence from individual differences and a neural network simulation. J. Exp. Psychol. Hum. Percept. Perform. 31 (3), 438–452.
Lezak, M.D., 2004. Neuropsychological Assessment. Oxford University Press, New York.
Li, B.J., Liu, L., Friston, K.J., Shen, H., Wang, L.B., Zeng, L.L., Hu, D.W., 2013. A treatment-resistant default mode subnetwork in major depression. Biol. Psychiatry 74 (1), 48–54.
Lidow, M.S., Goldmanrakic, P.S., Gallager, D.W., Geschwind, D.H., Rakic, P., 1989a. Distribution of major neurotransmitter receptors in the motor and somatosensory cortex of the rhesus-monkey. Neuroscience 32 (3), 609–627.
Lidow, M.S., Goldmanrakic, P.S., Gallager, D.W., Rakic, P., 1989b. Quantitative autoradiographic mapping of serotonin 5-Ht1 and 5-Ht2 receptors and uptake sites in the neocortex of the rhesus-monkey. J. Comp. Neurol. 280 (1), 27–42.
Lim, H.K., Juh, R., Pae, C.U., Lee, B.T., Yoo, S.S., Ryu, S.H., Kwak, K.R., Lee, C., Lee, C.U., 2008. Altered verbal working memory process in patients with Alzheimer's disease. Neuropsychobiology 57 (4), 181–187.
Loubinoux, I., Pariente, J., Boulanouar, K., Carel, C., Manelfe, C., Rascol, O., Celsis, P., Chollet, F., 2002a. A single dose of the serotonin neurotransmission agonist paroxetine enhances motor output: double-blind, placebo-controlled, fMRI study in healthy subjects. NeuroImage 15 (1), 26–36.
Loubinoux, I., Pariente, J., Rascol, O., Celsis, P., Chollet, F., 2002b. Selective serotonin reuptake inhibitor paroxetine modulates motor behavior through practice. A double-blind, placebo-controlled, multi-dose study in healthy subjects. Neuropsychologia 40 (11), 1815–1821.
Lu, H., Stein, E.A., 2014. Resting state functional connectivity: its physiological basis and application in neuropharmacology. Neuropharmacology 84, 79–89.
Maudoux, A., Lefebvre, P., Cabay, J.E., Demertzi, A., Vanhaudenhuyse, A., Laureys, S., Soddu, A., 2012a. Auditory resting-state network connectivity in tinnitus: a functional MRI study. PLoS One 7 (5), e36222.
Maudoux, A., Lefebvre, P., Cabay, J.E., Demertzi, A., Vanhaudenhuyse, A., Laureys, S., Soddu, A., 2012b. Connectivity graph analysis of the auditory resting state network in tinnitus. Brain Res. 1485, 10–21.
Mayberg, H.S., 1997. Limbic-cortical dysregulation: a proposed model of depression. J. Neuropsychiatr. Clin. Neurosci. 9 (3), 471–481.
McCabe, C., Mishor, Z., 2011. Antidepressant medications reduce subcortical–cortical resting-state functional connectivity in healthy volunteers. NeuroImage 57 (4), 1317–1323.
McCabe, C., Mishor, Z., Filippini, N., Cowen, P.J., Taylor, M.J., Harmer, C.J., 2011. SSRI administration reduces resting state functional connectivity in dorso-medial prefrontal cortex. Mol. Psychiatry 16 (6), 592–594.
McKie, S., Del-Ben, C., Elliott, R., Williams, S., del Vai, N., Anderson, I., Deakin, J.F.W., 2005. Neuronal effects of acute citalopram detected by pharmacoMRI. Psychopharmacology 180 (4), 680–686.
McRae, A., McRae, K., Brady, 2001. Review of sertraline and its clinical applications in psychiatric disorders. Expert. Opin. Pharmacother. 2 (5), 883–892.
Morgane, P.J., Galler, J.R., Mokler, D.J., 2005. A review of systems and networks of the limbic forebrain/limbic midbrain. Prog. Neurobiol. 75 (2), 143–160.
Morrison, J.H., Foote, S.L., Molliver, M.E., Bloom, F.E., Lidov, H.G., 1982. Noradrenergic and serotonergic fibers innervate complementary layers in monkey primary visual cortex: an immunohistochemical study. Proc. Natl. Acad. Sci. U. S. A. 79 (7), 2401–2405.
Murphy, S.E., Norbury, R., O'Sullivan, U., Cowen, P.J., Harmer, C.J., 2009. Effect of a single dose of citalopram on amygdala response to emotional faces. Br. J. Psychiatry 194 (6), 535–540.
Nichols, D.E., Nichols, C.D., 2008. Serotonin receptors. Chem. Rev. 108 (5), 1614–1641.
Niesters, M., Khalili-Mahani, N., Martini, C., Aarts, L., van Gerven, J., van Buchem, M.A., Dahan, A., Rombouts, S., 2012. Effect of subanesthetic ketamine on intrinsic functional brain connectivity: a placebo-controlled functional magnetic resonance imaging study in healthy male volunteers. Anesthesiology 117 (4), 868–877.
Norris, H., 1971. The action of sedatives on brain stem oculomotor systems in man. Neuropharmacology 10 (21), 181–191.
Oliveri, M., Calvo, G., 2003. Increased visual cortical excitability in ecstasy users: a transcranial magnetic stimulation study. J. Neurol. Neurosurg. Psychiatry 74 (8), 1136–1138.
Outhred, T., Hawkshead, B.E., Wager, T.D., Das, P., Malhi, G.S., Kemp, A.H., 2013. Acute neural effects of selective serotonin reuptake inhibitors versus noradrenaline reuptake inhibitors on emotion processing: implications for differential treatment efficacy. Neurosci. Biobehav. Rev. 37 (8), 1786–1800.
Peroutka, S.J., Snyder, S.H., 1979. Multiple serotonin receptors — differential binding of [5-hydroxytryptamine-H-3, [lysergic-H-3 acid diethylamide and [H-3]spiroperidol. Mol. Pharmacol. 16 (3), 687–699.
Rack-Gomer, A.L., Liu, T.T., 2012. Caffeine increases the temporal variability of resting-state BOLD connectivity in the motor cortex. NeuroImage 59 (3), 2994–3002.
Rack-Gomer, A.L., Liau, J., Liu, T.T., 2009. Caffeine reduces resting-state BOLD functional connectivity in the motor cortex. NeuroImage 46 (1), 56–63.
Reynell, C., Harris, J.J., 2013. The BOLD signal and neurovascular coupling in autism. Dev. Cogn. Neurosci. 6, 72–79.
Rijnbeek, B., De Visser, S., Franson, K., Cohen, A., Van Gerven, J., 2002. REM sleep reduction as a biomarker for the effects of antidepressants in healthy volunteers. Br. J. Clin. Pharmacol. 54 (5), 561–562.
Robinson, S., 2007. Antidepressants for treatment of tinnitus. Prog. Brain Res. 166, 263–271.
Rogers, M.A., Kasai, K., Koji, M., Fukuda, R., Iwanami, A., Nakagome, K., Fukuda, M., Kato, N., 2004. Executive and prefrontal dysfunction in unipolar depression: a review of neuropsychological and imaging evidence. Neurosci. Res. 50 (1), 1–11.
Sagud, M., Pivac, N., Muck-Seler, D., Jakovljevic, M., Mihaljevic-Peles, A., Korsic, M., 2002. Effects of sertraline treatment on plasma cortisol, prolactin and thyroid hormones in female depressed patients. Neuropsychobiology 45 (3), 139–143.
Schaefer, A., Burmann, I., Regenthal, R., Arelin, K., Barth, C., Pampel, A., Villringer, A., Margulies, D.S., Sacher, J., 2014. Serotonergic modulation of intrinsic functional connectivity. Curr. Biol. 24 (19), 2314–2318.
Seminowicz, D.A., Mayberg, H.S., McIntosh, A.R., Goldapple, K., Kennedy, S., Segal, Z., Rafi-Tari, S., 2004. Limbic-frontal circuitry in major depression: a path modeling metanalysis. NeuroImage 22 (1), 409–418.
Sheline, Y.I., Price, J.L., Yan, Z.Z., Mintun, M.A., 2010. Resting-state functional MRI in depression unmasks increased connectivity between networks via the dorsal nexus. Proc. Natl. Acad. Sci. U. S. A. 107 (24), 11020–11025.
Shima, K., Tanji, J., 1998. Role for cingulate motor area cells in voluntary movement selection based on reward. Science 282 (5392), 1335–1338.
Smith, S.M., 2002. Fast robust automated brain extraction. Hum. Brain Mapp. 17 (3), 143–155.
Smith, S.M., Nichols, T.E., 2009. Threshold-free cluster enhancement: addressing problems of smoothing, threshold dependence and localisation in cluster inference. NeuroImage 44 (1), 83–98.
Smith, G.S., Ma, Y., Dhawan, V., Gunduz, H., Carbon, M., Kirshner, M., Larson, J., Chaly, T., Belakhleff, A., Kramer, E., Greenwald, B., Kant, J.M., Laghrissi-Thode, F., Pollock, B.G., Eidelber, D., 2002. Serotonin modulation of cerebral glucose metabolism measured with positron emission tomography (PET) in human subjects. Synapse 45 (2), 105–112.
Smith, S.M., Jenkinson, M., Woolrich, M.W., Beckmann, C.F., Behrens, T.E.J., Johansen-Berg, H., Bannister, P.R., De Luca, M., Drobnjak, I., Flitney, D.E., Niazy, R.K., Saunders, J., Vickers, J., Zhang, Y.Y., De Stefano, N., Brady, J.M., Matthews, P.M., 2004. Advances in functional and structural MR image analysis and implementation as FSL. NeuroImage 23 (Suppl. 1), S208–S219.
Smith, S.M., Fox, P.T., Miller, K.L., Glahn, D.C., Fox, P.M., Mackay, C.E., Filippini, N., Watkins, K.E., Toro, R., Laird, A.R., Beckmann, C.F., 2009. Correspondence of the brain's functional architecture during activation and rest. Proc. Natl. Acad. Sci. U. S. A. 106 (31), 13040–13045.
Stroop, J.R., 1935. Studies of interference in serial verbal reactions. J. Exp. Psychol. 18, 643–662.
Sundermann, B., Beverborg, M.O.L., Pfleiderer, B., 2014. Toward literature-based feature selection for diagnostic classification: a meta-analysis of resting-state fMRI in depression. Front. Hum. Neurosci. 692 (8).
Thompson, G.C., Thompson, A.M., Garrett, K.M., Britton, B.H., 1994. Serotonin and serotonin receptors in the central auditory-system. Otolaryngol. Head Neck Surg. 110 (1), 93–102.

Ueyama, T., Donishi, T., Ukai, S., Ikeda, Y., Hotomi, M., Yamanaka, N., Shinosaki, K., Terada, M., Kaneoke, Y., 2013. Brain regions responsible for tinnitus distress and loudness: a resting-state fMRI study. PLoS One 8 (6), e67778.

van de Ven, V., Wingen, M., Kuypers, K.P.C., Ramaekers, J.G., Formisano, E., 2013. Escitalopram decreases cross-regional functional connectivity within the default-mode network. PLoS One 8 (6), e68355.

van Wingen, G.A., Tendolkar, I., Urner, M., van Marle, H.J., Denys, D., Verkes, R.J., Fernandez, G., 2014. Short-term antidepressant administration reduces default mode and task-positive network connectivity in healthy individuals during rest. NeuroImage 88, 47–53.

Veer, I.M., Oei, N.Y.L., Spinhoven, P., van Buchem, M.A., Elzinga, B.M., Rombouts, S.A.R.B., 2012. Endogenous cortisol is associated with functional connectivity between the amygdala and medial prefrontal cortex. Psychoneuroendocrinology 37 (7), 1039–1047.

Viviani, R., Abler, B., Seeringer, A., Stingl, J.C., 2012. Effect of paroxetine and bupropion on human resting brain perfusion: an arterial spin labeling study. NeuroImage 61 (4), 773–779.

Vogt, B.A., Finch, D.M., Olson, C.R., 1992. Functional heterogeneity in cingulate cortex: the anterior executive and posterior evaluative regions. Cereb. Cortex 2 (6), 435–443.

von Bardeleben, U., Steiger, A., Gerken, A., Holsboer, F., 1989. Effects of Fluoxetine upon pharmacoendocrine and sleep-EEG parameters in normal controls. Int. Clin. Psychopharmacol. 4, 1–5.

Wechsler, D., 1981. The psychometric tradition — developing the Wechsler Adult Intelligence Scale. Contemp. Educ. Psychol. 6 (2), 82–85.

Whale, R., Clifford, E.M., Bhagwagar, Z., Cowen, P.J., 2001. Decreased sensitivity of 5-HT1D receptors in melancholic depression. Br. J. Psychiatry 178, 454–457.

Winkler, A.M., Ridgway, G.R., Webster, M.A., Smith, S.M., Nichols, T.E., 2014. Permutation inference for the general linear model. NeuroImage 92, 381–397.

Wong, C.W., Olafsson, V., Tal, O., Liu, T.T., 2012. Anti-correlated networks, global signal regression, and the effects of caffeine in resting-state functional MRI. NeuroImage 63 (1), 356–364.

Woolrich, M.W., Jbabdi, S., Patenaude, B., Chappell, M., Makni, S., Behrens, T., Beckmann, C., Jenkinson, M., Smith, S.M., 2009. Bayesian analysis of neuroimaging data in FSL. NeuroImage 45 (Suppl. 1), S173–S186.

Zhang, S., Li, C.S.R., 2012. Functional connectivity mapping of the human precuneus by resting state fMRI. NeuroImage 59 (4), 3548–3562.

Zhu, X.L., Wang, X., Xiao, J., Liao, J., Zhong, M.T., Wang, W., Yao, S.Q., 2012. Evidence of a dissociation pattern in resting-state default mode network connectivity in first-episode, treatment-naive major depression patients. Biol. Psychiatry 71 (7), 611–617.